X-ray emission spectra induced by ion-atom collisions I : single and double K-shell ionization

Kawatsura, Kiyoshi

X-RAY EMISSION SPECTRA INDUCED BY ION-ATOM COLLISIONS I

Single and Double K-Shell Ionization

BY KIYOSHI KAWATSURA

Experimental cross sections were determined for the single and double K-shell ionization of Be, B and O atoms by H (0.3–2.0 MeV), He (0.25–2.0 MeV), N (0.3–1.1 MeV) and Ar (0.3–1.8 MeV) ion bombardments using a high resolution Bragg spectrometer.

The results of the single K-shell ionization for H and He ion bombardments showed a good agreement with the calculated result by the Coulomb excitation of the binary-encounter approximation (BEA), while those of the heavy ion bombardments were understood in terms of the electron promotion model.

The cross sections of the double K-shell ionization for the H and He ion bombardments were for the first time measured, and the results showed that the cross section was dependent on Z_1^4 of the projectile nuclear charge and a maximum cross section was obtained at $E/\mathcal{U}'=1$.

Introduction

Recently, numerous studies of the inner-shell ionization resulting from ion-atom collisions have led to the discovery of a wide variety of interesting new phenomena[1,2]. Much of these efforts has been directed to elucidate the various mechanisms by which inner-shell vacancies are produced during the collision process. For light ions such as hydrogen and helium ions, the mechanism of the inner-shell vacancy production is explained by the direct Coulomb excitation theory. In heavy ion collisions, on the other hand, the cross sections of inner-shell ionization are often very high and strongly depend on the matching of energy levels in the collision partners. The experimental data can be interpreted in terms of electron promotion model[3,4].

One of the most striking phenomena in inner-shell vacancy production by the bombardment of the heavy charged particles is the high degree of multiple inner-shell ionization. There have been observations by several groups of satellite and hypersatellite X-ray spectra using high resolution spectrometers. Specifically, the satellite peaks of K-shell correspond to removing 1 K- and n L-shell electrons (n=0, 1,……, 8) and the hypersatellite peaks to removing 2 K- and n L-shell electrons.

(*Received September 25, 1977*)

1) J. D. Garcia, R. J. Fortner and T. M. Kavanagh, *Rev. Mod. Phys.*, **45**, 111 (1973)
2) P. Richard, "Atomic Inner-Shell Processes", edited by B. Crasemann, Vol. 1, p. 73, Academic Press, New York (1975)
3) U. Fano and W. Lichten, *Phys. Rev. Lett.*, **14**, 627 (1965)
4) J. S. Briggs and J. Macek, *J. Phys.*, **B5**, 579 (1972)

The Review of Physical Chemistry of Japan Vol. 47 No. 2 (1977)

For the double K-shell ionization process, Olsen and Moore[5] investigated oxygen ion bombardment on Ca target at very high energy. Recently, Nagel *et al.*[6] have measured K^2 hypersatellite X-ray energies from Be to Ne by heavy ion bombardments and Kawatsura *et al.*[7-10] reported energy dependence of the double K-shell ionization cross sections of the light elements by hydrogen and helium ion bombardments.

In the present work, we report an extensive investigation of the K X-ray spectra of the Be, B and O atoms observed from the thick Be, B and BeO targets, respectively, by bombardment with H^+, H_2^+, He^+, N^+, Ar^+ and Ar^{2+} ions in the energy range of 0.25 to 2.0 MeV. We have also measured the energy dependence of the absolute cross sections for the single and double K-shell ionization by the same projectile ions. The measured cross sections were compared with the available theoretical calculations. Measurements of the K X-ray spectra have been performed on a number of the thick solid targets using the H, He, N and Ar ion beams from a 2-MV Van de Graaff accelerator. H, He, N and Ar ions denote H^+ and H_2^+, He^+, N^+, and Ar^+ and Ar^{2+} ions, respectively.

Theoretical Considerations

Atomic inner-shell vacancy production by H or He ion bombardment is caused by the direct Coulomb excitation. The cross section for K-shell ionization can be explained with some success by the theoretical calculations. These are the plane-wave Born approximation (PWBA), the semiclassical Coulomb approximation (SCA) and the binary-encounter approximation (BEA).

Plane-wave Born approximation

Merzbacher and Lewis[11] and Basbas *et al.*[12] presented the extended discussions of the inner-shell ionization process using the PWBA to make the quantum mechanical calculations. In this model, the Coulomb potential of the incoming particle is considered as a perturbation which produces the atomic transition, and the projectile is considered as a plane wave both before and after the impact. The K-shell ionization cross section is given by

$$\sigma_1=(\sigma_{0K}/\theta_K)f(\eta_K/\theta_K^2), \quad (1)$$

5) D. K. Olsen and C. F. Moore, *Phys. Rev. Lett.*, **33**, 194 (1974)
6) D. J. Nagel, A. R. Knudson and P. G. Burkhalter, *J. Phys.*, **B8**, 2779 (1975)
7) K. Kawatsura, K. Ozawa, F. Fujimoto and M. Terasawa, "Ion Beam Surface Layer Analysis", edited by O. Meyer, G. Linker and F. Käppeler, Vol. 2, p. 719, Plenum Press, New York (1976)
8) F. Fujimoto, K. Kawatsura, K. Ozawa and M. Terasawa, *Phys. Lett.*, **A57**, 263 (1976)
9) K. Kawatsura, K. Ozawa, F. Fujimoto and M. Terasawa, *Phys. Lett.*, **A58**, 446 (1976)
10) K. Kawatsura, K. Ozawa, F. Fujimoto and M. Terasawa, *Proc. 10th Int. Conf. on Physics of Electronic and Atomic Collisions, (Paris), Abstracts* p. 50, (1977) and to be published in *Phys. Lett., A*
11) E. Merzbacher and H. W. Lewis, "Handbuch der Physik," edited by S. Flügge, Vol. 34, p. 166, Springer-Verlag, Berlin (1958)
12) G. Basbas, W. Brandt and R. Laubert, *Phys. Rev.*, **A7**, 983 (1973)

The Review of Physical Chemistry of Japan Vol. 47 No. 2 (1977)

where

$$\sigma_{0K}=8\pi(Z_1/Z_{2K}^2)^2a_0^2, \qquad \theta_K=U/Z_{2K}^2Ry,$$
$$\eta_K=Z_{2K}^2Ry(m/M)E, \qquad Z_{2K}=Z_2-0.3,$$

and where Z_1 and Z_2 are the nuclear charges of the projectile ion and the target atom, respectively, E is the incident energy of the projectile ion, U is the binding energy of the K-shell electron, Ry is the Rydberg constant, m and M are the masses of an electron and the projectile, a_0 is the Bohr radius and $f(\eta_K/\theta_K^2)$ is a universal function of η_K/θ_K^2 given by Basbas *et al.*[12] This formalism as well as the SCA and the BEA predicts a simple scaling relationship for the collisions between different ion-atom pairs as the collision velocity changes.

Semiclassical Coulomb approximation

Bang and Hansteen[13] in 1959 employed an impact parameter formalism to account for the deflection of the incident ion by the target atom. In this theory, the ionization is considered to be due to the time dependent perturbation of the incoming particle which describes a classical trajectory. The SCA was shown to be equivalent to the PWBA for the identical limiting conditions. There was a good agreement with experiment at lower energies. However, the present work was done in the high energy region, so we did not carry out the theoretical calculation using the SCA.

Binary-encounter approximation

In 1965 Gryzinski[14] made new calculations on the classical collision theories using the binary-encounter approximation (BEA). The BEA gives ionization probabilities by considering the direct interaction between the incident ion and the electrons of the target atom and disregarding the mutual interaction between the atomic electron and the nucleus during the collision. Moreover, in 1970 Garcia[15] obtained an excellent agreement between experiments and the BEA, and proposed a following universal ionization curve :

$$\sigma_I=(Z_1^2/U^2)f(E/\lambda U). \qquad (2)$$

Here $f(E/\lambda U)$ is a universal function depending only on $E/\lambda U$, and λ is the mass ratio of the projectile ion to electron.

We have calculated relevant K-shell ionization cross sections using the PWBA and BEA formalism in order to compare with the experimental results obtained. The tables of Khandelwal *et al.*[16] were used in the PWBA calculations, while the BEA results were scaled from the universal curve of Garcia[15].

Experimentals

The experiments were carried out with the use of ion beams from a 2-MV Van de Graaff ac-

13) J. Bang and J. M. Hansteen, *K. Dan. Vidensk. Selsk. Mat.-Fys. Medd.*, **31**, No. 13 (1959)
14) M. Gryzinski, *Phys. Rev.*, **138**, A336 (1965)
15) J. D. Gracia, *Phys. Rev.*, **A1**, 280 (1970)
16) G. S. Khandelwal, B. H. Choi and E. Merzbacher, *At. Data*, **1**, 103 (1969)

The Review of Physical Chemistry of Japan Vol. 47 No. 2 (1977)

celerator of Japan Atomic Energy Research Institute. The ion beams were deflected through an energy and momentum analyzing magnet and focused on the thick solid targets vertically by means of a set of quadrupole magnets and a series of collimators. The diameter of the beam spot was mainly 0.8 mm. X-rays were detected at a take-off angle of 45° by a gas-flow type proportional counter with a 1.0 μ thick polypropylene window. The counter was operated in flow mode of 55 cc/min utilizing P-75 gas (25% argon and 75% methane) at atmospheric pressure for Be, B and O K X-ray detection, because this ratio of a gas mixture has shown better energy resolution for measuring low energy X-rays than any other ratios of these two gases. The proportional counter pulses were discriminated by a single-channel pulse-height analyzer and counted by an electronic scaler, which was gated by a target current integrator.

The detailed study of K_α satellite and hypersatellite spectra requires the use of a high-resolution crystal diffraction spectrometer. The schematic diagrams of the experimental configuration are shown in Figs. 1 and 2. The system employed in the present work was a flat crystal Bragg spectrometer which had two Soller slits with dispersion angles of 0.5° and 0.86°, respectively. The measurements of K_α and $K_\alpha{}^2$ X-ray spectra from the Be atoms were performed with a pseudo-crystal of the lead-lignocerate soap film with 100 layers ($2d$ spacing=130 Å) and the measurements of K_α and $K_\alpha{}^2$ X-ray spectra from the B atoms and $K_\alpha{}^2$ X-ray spectra from the Be atoms were performed with a pseudo-crystal of the lead-stearate soap film with 100 layers ($2d$ spacing=100 Å) and the measurements of K_α and $K_\alpha{}^2$ X-ray spectra from the O atoms were performed with a single crystal of rubidium hydrogen phthalate ($2d$ spacing=26.1 Å). The experimental energy resolutions (full width at half maximum) of the K_α X-ray peak were 6.1, 5.4 and 4.1 eV for the Be, B and O atoms,

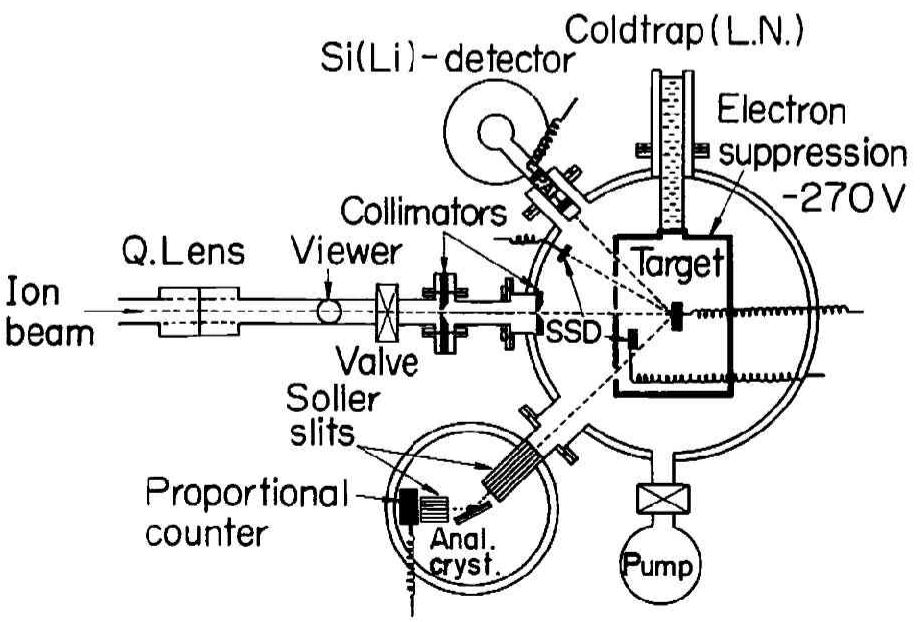

Fig. 1 Schematic diagram of experimental arrangement for X-ray spectrum measurement

The Review of Physical Chemistry of Japan Vol. 47 No. 2 (1977)

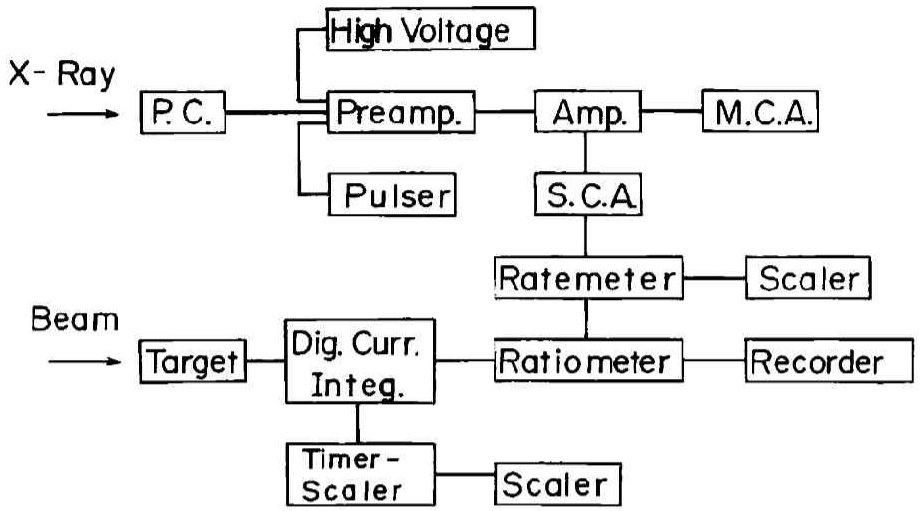

Fig. 2 The detector set-up and electronics

respectively.

The high resolution measurement using a diffraction spectrometer is useful for correcting non-dispersion data because in heavy ion-atom collisions X-rays are sometimes generated from the projectile ions and are not resolved by the proportional counter alone from the X-rays of the target atoms. This measurement is also useful for obtaining new and more specific informations concerning the mechanism of the inner-shell ionization and the effect of the chemical bonding on the X-ray spectra produced in heavy ion-atom collisions.

Results and Discussions

K_α diagram and K_α^2 hypersatellite X-ray spectra

Fig. 3 shows the K X-ray spectra of Be induced by 0.3 MeV H^+ and 1.2 MeV He^+ ion bombardments, where the velocities of each ion are the same. The main peaks at 108.5 eV in both spectra are the K_α diagram lines due to the single K-shell ionization. For the He^+ ion bombardment, the second peak arising from the double K-shell ionization was observed at 146.1 eV. Its width was about 10 eV which was about twice of that of the main peak. It is noticeable that the peak due to the double K-shell ionization in H^+ ion bombardment is not observable in the energy range of the present experiment. Fig. 4 shows the K X-ray spectra of B induced by 1.5 MeV H^+ and He^+ ion bombardment. The main peaks at about 183 eV in both spectra are the K_α diagram lines from the B atoms. In this case, the second peak arising from the double K-shell ionization was also observed at 230.8 eV for the He^+ ion bombardment. The transition energies of the K_α diagram and K_α^2 hypersatellite lines from the Be and B atoms are in good agreement with the results of the other measurements and theoretical calculations[6-8]. Fig. 5 shows the K X-ray spectra of the O atoms in BeO

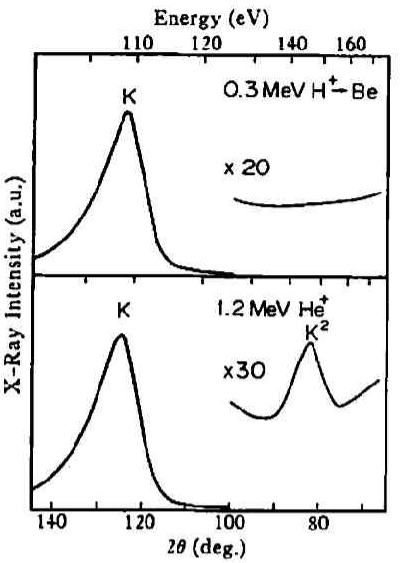

Fig. 3 K X-ray spectra of Be induced by 0.3 MeV H^+ and 1.2 MeV He^+ ion bombardment

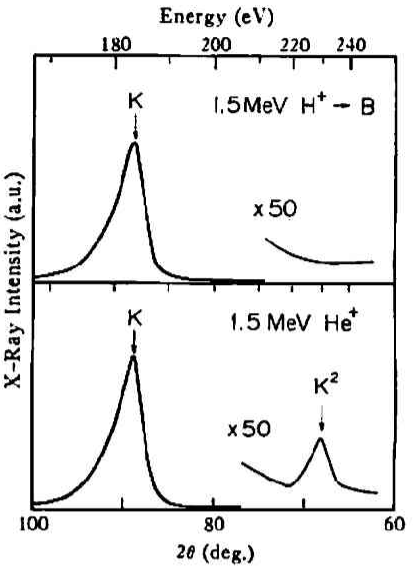

Fig. 4 K X-ray spectra of B induced by 1.5 MeV H^+ and 1.5 MeV He^+ ion bombardment

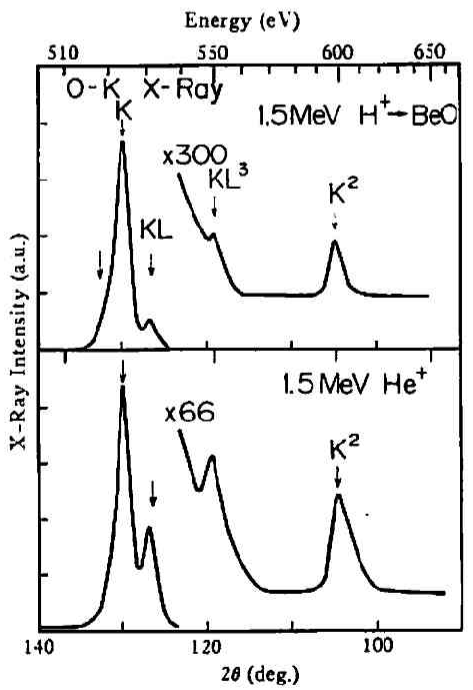

Fig. 5 K X-ray spectra of O induced by 1.5 MeV H^+ and 1.5 MeV He^+ ion bombardment on thick BeO target

target induced by 1.5 MeV H^+ and He^+ ion bombardments. In this case, the spectra observed are

more complicated than those from the Be and B targets. The main peaks at 525 eV in both spectra are the K_α diagram lines due to the single K-shell ionization in the O atom. The satellite peaks are observable at 532 eV and 550 eV in both spectra. They can be identified as the KL and KL^3 satellite transitions from the O atoms with the 1 K- and 1 L-shell, and the 1 K- and 3 L-shell vacancies, respectively. The details will be discussed later. A clear peak is observed at 600 eV for H^+ and 602 eV for He^+ ion bombardments, respectively. They can be also identified as the $K_\alpha{}^2$ hypersatellite transition from the O atoms with the double K-shell vacancies and the transition energy is in good agreement with the other measurements and theoretical calculations[6,9,17]. This is the first case where the hypersatellite line is observed for the H^+ ion bombardment.

Using the step scanning method, we have tried to extend the measurements of the $K_\alpha{}^2$ hypersatellite X-rays from the Be, B and O atoms by bombardments of H^+, $H_2{}^+$ and He^+ ions[10]. We have confirmed that the single and double K-shell ionization cross sections by $H_2{}^+$ ion bombardment were also the same as those by H^+ ion bombardment at a fixed velocity, so in this experiment we have employed the $H_2{}^+$ ion beam as the projectile of $Z_1=1$ because $H_2{}^+$ ion beam with the same velocity as He^+ ion beam was easily generated with higher intensity and better stability than the H^+ ion beam. Fig. 6 shows the Be K^2 X-ray spectra induced by 0.8 MeV $H_2{}^+$ and 1.6 MeV He^+ ion

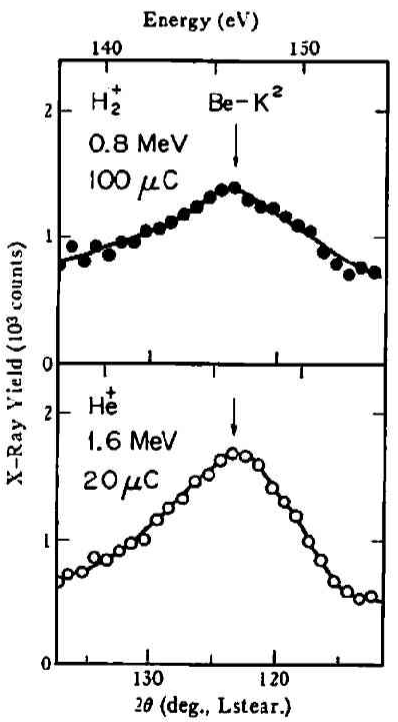

Fig. 6 K^2 X-ray spectra of Be induced by 0.8 MeV $H_2{}^+$ and 1.6 MeV He^+ ion bombardment

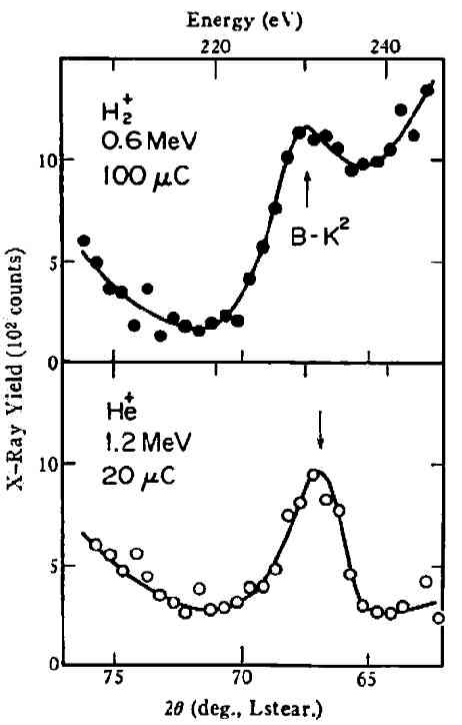

Fig. 7 K^2 X-ray spectra of B induced by 0.6 MeV $H_2{}^+$ and 1.2 MeV He^+ ion bombardment

17) H. Kamada and M. Terasawa, *Anal. Chim. Acta*, **17**, 303 (1974)

bombardments, where the velocities of each ion are the same, *i. e.*, $E/\lambda U=1.96$, so it is convenient to compare the experimental results with the theoretical calculations. In the case of the H_2^+ ion bombardment, it is evident that the double K-shell ionization cross section is very small, that is, about 1/18 of that for the He^+ ion bombardment. The similar spectra are also obtained for a variety of the scaled velocity. Fig. 7 shows the B K^2 X-ray spectra induced by 0.6 MeV H_2^+ and 1.2 MeV He^+ ion bombardments where $E/\lambda U=0.87$. In the case of the H_2^+ ion bombardments, the B K^2 X-ray line is observable at about 230 eV, but a quantitative analysis is difficult because the cross section decreases with the increase of the incident energy of the H_2^+ ion in the present energy range, in addition to the overlapping with the low energy tail of the C K X-ray band due to the surface contamination. Fig. 8 shows the O K^2 X-ray spectra induced by 0.8 MeV H_2^+ and 1.6 MeV He^+ ion bombardment where $E/\lambda U=0.41$. The ratio of the cross section of the double K-shell ionization for the He ion to that for the H ion, $\sigma_{2K}(He)/\sigma_{2K}(H)$, is found to be about 14. These facts suggest that the cross section of the double K-shell ionization, σ_{2K} is represented as a function of Z_1^4 and $E/\lambda U$, and in this case, it means that $\sigma_{2K}(He)/16\sigma_{2K}(H)$ is equal to unity.

Single K-shell ionization cross section

In order to obtain the absolute cross sections from the observed X-ray spectra and non-dispersive X-ray yields, the following procedures were carried out.

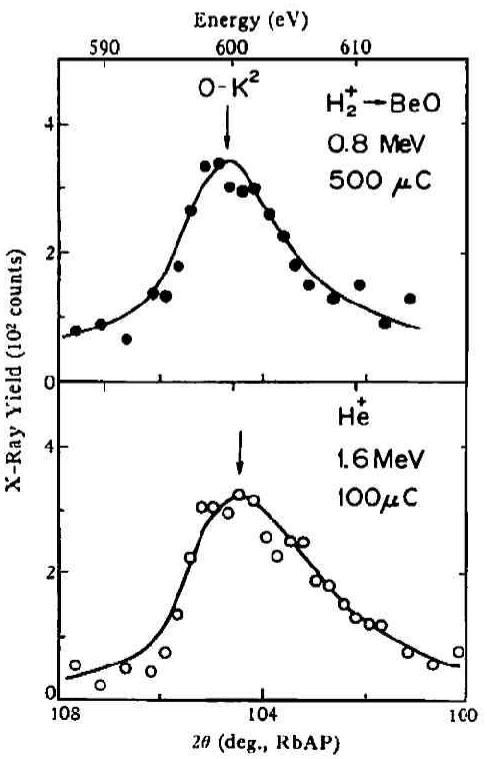

Fig. 8 K^2 X-ray spectra of O induced by 0.8 MeV H_2^+ and 1.6 MeV He^+ ion bombardment

Thick target yield $Y(E)$ was obtained from the directly measured X-ray counts by considering the corrections for incident ion flux, geometry factor, window absorption, detector efficiency and reflection efficiency of analyzing crystal. In argon ion bombardment, Ar^{2+} ions together with Ar^{+} ions were also employed to extend the incident energy range. The results for a given incident ion kinetic energy were shown to be independent of the initial charge state of the ion. The X-ray production cross section $\sigma_X(E)$ was calculated from a thick target yield $Y(E)$ by the relation:

$$\sigma_X(E)=\frac{1}{n}\left\{\frac{dY(E)}{dE}S(E)+\frac{\mu\,\mathrm{cosec}(\pi/4)}{\rho}Y(E)\right\}, \tag{3}$$

where $S(E)$ is the total stopping power for the incident ion in the target material, n is the density of the target atoms and μ/ρ is the target absorption coefficient for the K_α or $K_\alpha{}^2$ X-rays. $S(E)$ is equal to the sum of the nuclear stopping power $S_n(E)$ and the electronic stopping power $S_e(E)$. In the case of the light ion such as H or He ion, $S_n(E)$ can be neglected in the present energy range and $S_e(E)$ is quoted and interpolated from the data of Northcliffe and Schilling[18]. The $S_n(E)$ for the heavy ions was calculated from the theory presented by Lindhard, Scharff and Schiøtt[19]. The absorption coefficients were taken from the data of Henke and Elgin[20]. The derivative of the X-ray

Table 1. Experimental data of X-ray production and K-shell ionization cross sections together with absorption coefficients (cm^2/g) and fluorescence yields. In this notation, 2.53 (−21) = 2.53×10^{-21}

Be-K	μ/ρ=5.31 (3)	ω=3.04 (−4)	Be-K²	μ/ρ=1.00 (5)	
E (MeV)	σ_X (cm^2)	σ_I (cm^2)	E (MeV)	σ_X (cm^2)	σ_I (cm^2)
H			H		
0.30	2.53 (−21)	8.34 (−18)	0.30	1.84 (−22)	6.06 (−19)
0.50	2.26	7.43	0.40	1.20	3.95
0.70	2.00	6.56	0.50	8.64 (−23)	2.84
1.00	1.68	5.57	0.60	6.59	2.17
1.20	1.61	5.30	0.70	5.18	1.70
1.50	1.52	4.98	0.80	4.31	1.42
1.80	1.42	4.67	0.90	3.64	1.20
He			He		
0.25	6.09 (−21)	2.00 (−17)	0.30	8.02 (−22)	2.64 (−18)
0.30	7.28	2.40	0.50	2.13 (−21)	7.02
0.50	1.10 (−20)	3.62	0.60	2.64	8.70
0.80	1.11	3.66	0.80	3.13	1.03 (−17)
1.00	1.07	3.52	1.00	3.03	9.98 (−18)
1.20	1.02	3.35	1.20	2.70	8.87
1.50	9.62 (−21)	3.17	1.50	2.11	6.94
1.80	8.91	2.93	1.80	1.51	4.95
2.00	8.22	2.70	2.00	1.35	4.44

18) L. C. Northcliffe and R. F. Schilling, *Nucl. Data Tables*, **7**, 233 (1970)

19) J. Lindhard, M. Scharff and H. E. Schiøtt, *K. Dan. Vidensk. Selsk. Mat.-Fys. Medd.*, **33**, No. 14 (1963)

20) B. L. Henke and R. L. Elgin, *Advances in X-Ray Analysis*, **13**, 639 (1970)

Table 1. (Continued)

B–K	μ/ρ=3.35 (3)	ω=7.10 (−4)	B–K²	μ/ρ=5.70 (4)	
E (MeV)	σ_X (cm²)	σ_I (cm²)	E (MeV)	σ_X (cm²)	σ_I (cm²)
H			H		
0.50	1.51 (−21)	2.13 (−18)	0.30	3.75 (−23)	5.28 (−20)
0.75	1.43	2.01	0.40	4.05	5.70
1.00	1.32	1.87	0.50	3.59	5.06
1.20	1.23	1.74			
1.40	1.14	1.61			
1.60	1.07	1.50			
1.80	1.01	1.42			
2.00	9.78 (−22)	1.38			
He			He		
0.50	4.06 (−21)	5.71 (−18)	0.50	1.48 (−22)	2.08 (−19)
0.75	5.43	7.64	0.75	3.90	5.49
1.00	6.29	8.85	1.00	6.02	8.48
1.25	6.88	9.69	1.25	7.17	1.01 (−18)
1.50	7.15	1.01 (−17)	1.50	7.86	1.11
1.75	7.11	1.00	1.75	5.59	7.88 (−19)
2.00	6.82	9-61 (−18)	2.00	3.84	5.40

Table 1. (Continued)

O–K	μ/ρ=1.21 (3)	ω=6.45 (−3)	O–K²	μ/ρ=1.68 (4)	
E (MeV)	σ_X (cm²)	σ_I (cm²)	E (MeV)	σ_X (cm²)	σ_I (cm²)
H			H		
0.45	1.63 (−21)	2.52 (−19)	0.45	5.85 (−24)	9.07 (−22)
0.60	1.60	2.49	0.60	8.81	1.37 (−21)
0.80	1.79	2.78	0.80	1.15 (−23)	1.78
1.00	1.77	2.74	1.00	1.30	2.02
1.40	1.67	2.58	1.40	1.33	2.05
1.80	1.58	2.46	1.80	1.27	1.97
He			He		
0.60	1.26 (−21)	1.95 (−19)	0.60	5.42 (−24)	8.40 (−22)
0.90	2.90	4.49	0.90	1.83 (−23)	2.84 (−21)
1.20	4.34	6.73	1.20	3.96	6.14
1.50	5.45	8.46	1.50	7.60	1.18 (−20)
1.80	6.43	9.98	1.80	1.11 (−22)	1.72

yield function was obtained analytically from the least squares polynomial fits to the experimental yield curve. The K-shell ionization cross section σ_I is related to σ_X by

$$\sigma_X=\omega_K\sigma_I, \tag{4}$$

Table 2. Experimental data of X-ray production and K-shell ionization cross sections together with absorption coefficients (cm^2/g) and fluorescence yield

B-K	μ/ρ=3.35 (3)	ω=7.10 (−4)	B-K²	μ/ρ=5.70 (4)	
E (MeV)	σ_X (cm^2)	σ_I (cm^2)	E (MeV)	σ_X (cm^2)	σ_I (cm^2)
N			N		
0.30	2.74 (−21)	3.86 (−18)	0.30	7.64 (−22)	1.08 (−18)
0.50	3.52	4.96	0.50	1.28 (−21)	1.80
0.70	4.23	5.95	0.70	1.71	2.41
0.90	4.85	6.82	0.90	2.08	2.93
1.10	5.53	7.79	1.10	2.51	3.54
Ar			Ar		
0.30	7.25 (−21)	1.02 (−17)	0.30	6.42 (−22)	9.04 (−19)
0.45	8.10	1.14	0.45	9.23	1.30 (−18)
1.00	1.21 (−20)	1.71	1.00	1.98 (−21)	2.79
1.40	1.23	1.73	1.40	2.58	3.64
1.80	1.12	1.57	1.80	2.88	4.05

where ω_K is the K-shell fluorescence yield whose values are given by Dick and Lucas[21] and Tawara *et al.*[22] The fluorescence yield for the double K-shell ionization, ω_{2K}, are not so well known. However, the calculation by Bhalla and Hein[23] indicates, for Ne, that the ratio of fluorescence yields, ω_{2K}/ω_{1K}, is nearly equal to unity if the number of the L-shell vacancies is the same. We assume this is the case for Be, B and O atoms and apply the same values to the double K-shell ionization. The used values of μ/ρ and ω_K are listed in Tables 1 and 2. The uncertainty in the absolute cross sections of the K-shell ionization is within a factor of 2.

The experimental cross sections for the single and double K-shell ionization of Be, B and O obtained from the thick target X-ray yield are also summarized in Table 1, and shown in Figs. 9, 10 and 11 together with the theoretical predictions for the single K-shell ionization. The solid curve represents the theoretical cross section for the single K-shell ionization predicted by the BEA and the dashed curve represents that predicted by the PWBA. Generally, the BEA can better reproduce the experimental cross sections except at high energies ($E/\lambda U \geq 3.0$) where the PWBA gives a better fit to the observed results than the BEA. As described before, the BEA theory results in the following scaled equation for the single K-shell ionization cross sections; $\sigma_{1K}=(Z_1^2/U^2)f(E/\lambda U)$. The important point is that a plot of $U^2\sigma_{1K}/Z_1^2$ as a function of $E/\lambda U$ should yield a universal curve for various projectile ions and target atoms. In Fig. 12, we show the comparison between the universal curve of the BEA theory by Garcia[15] and the experimental single K-shell ionization cross sections for H and He ion bombardments on the thick Be, B and O (BeO) targets. The results presented here

21) C. E. Dick and A. C. Lucas, *Phys. Rev.*, A2, 580 (1970)

22) H. Tawara, K. G. Harrison and F. J. de Heer, *Physica*, 63, 351 (1973)

23) C. P. Bhalla and M. Hein, *Phys. Rev. Lett.*, 30, 39 (1973)

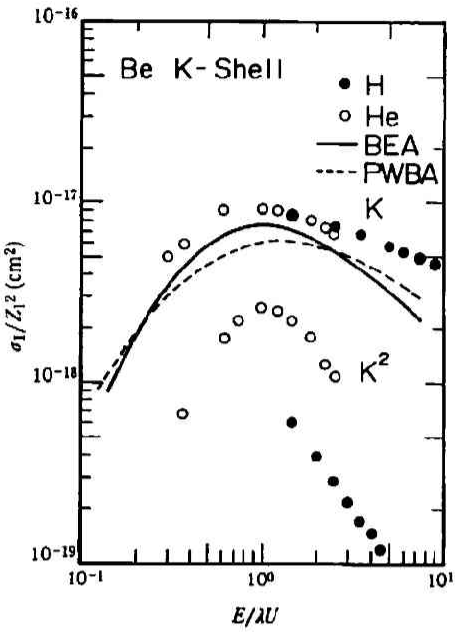

Fig. 9 Single and double K-shell ionization cross sections of Be for H and He ion bombardment. The solid curve is the BEA calculations and the dashed curve the PWBA calculations

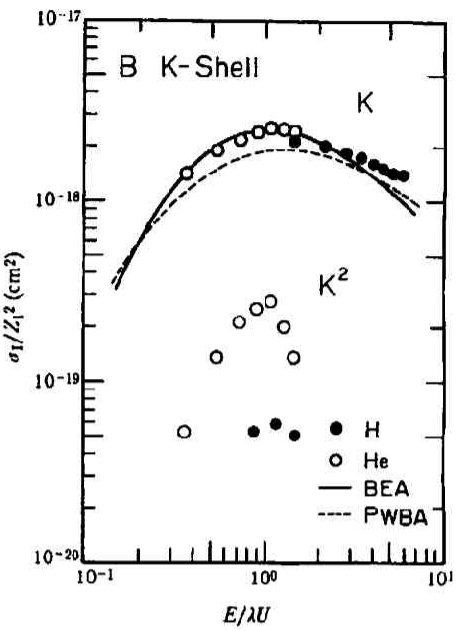

Fig. 10 Single and double K-shell ionization cross sections of B for H and He ion bombardment. The solid curve is the BEA calculations and the dashed curve the PWBA calculations

indicate that the BEA theory provides a useful approach to predict the K-shell ionization cross sections for a wide range of the target atoms and of the H and He ion energies where $0.1 \leq E/\lambda U \leq 5.0$. The ease with which the calculated cross sections may be scaled for the different bombarding energies and target atoms presents a reasonable case for the use of this formalism in application such as trace element analysis by charged particle bombardment.

Double K-shell ionization cross section

In the case of the double K-shell ionization by the direct Coulomb excitation, the several reports[24-27] have recently considered the theoretical calculations using the SCA or the BEA. It is common to consider the scattering of the particles as a function of the impact parameter b and to express the total cross section as an integral over the impact parameter, namely,

$$\sigma_{1K} = 2\int 2\pi b P_K(E, b) db. \tag{5}$$

where $P_K(E, b)$ is the probability of ionizing a single electron from the K-shell. According to the

24) J. M. Hansteen and O. P. Mosebekk, *Phys. Rev. Lett.*, **29**, 1361 (1972)
25) J. H. McGuire and P. Richard, *Phys. Rev.*, **A8**, 1374 (1973)
26) J. S. Hansen, *Phys. Rev.*, **A8**, 822 (1973)
27) J. H. McGuire, *At. Data Nucl. Data Tables*, **13**, 491 (1974)

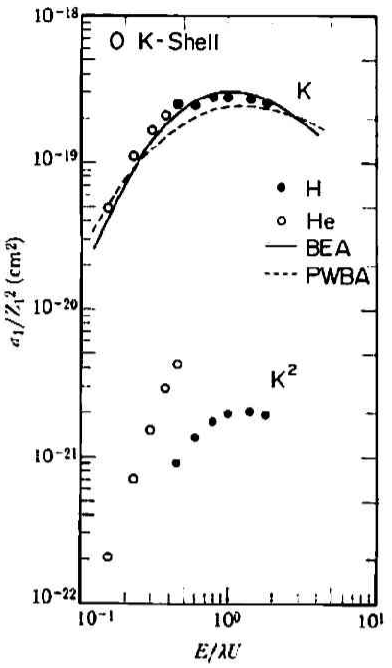

Fig. 11 Single and double K-shell ionization cross sections of O for H and He ion bombardment. The solid curve is the BEA calculations and the dashed curve the PWBA calculations

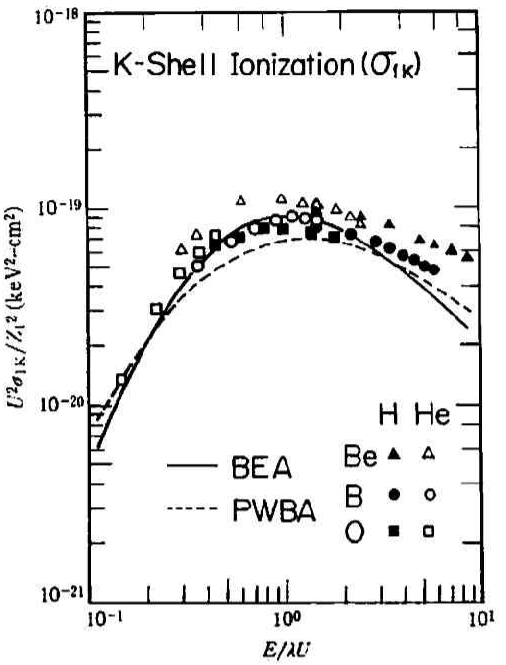

Fig. 12 Comparison of the single K-shell ionization cross sections of light elements for H and He ion bombardment with the scaled universal BEA curve and PWBA curve

classical treatment, the probability of ionizing several electrons is proportional to the product of the individual probabilities. Hence, the cross section for the double K-shell ionization is given by

$$\sigma_{2K}=\int 2\pi b[P_K(E, b)]^2 db. \qquad (6)$$

Using the density distribution corresponding to identical electrons in a filled hydrogenic shell, $P(E, b)$ is essentially independent of the mass of the projectile ion, that is, $P(E, b)=P(v, b)$, where $v=(E/\lambda U)^{1/2}$. The resulting $P(v, b)$ obeys the scaling law: $P_{Z_1}(v, b)=Z_1^2 P_{Z_1=1}(v, b)$. Since $P(v, b)$ does not depend on the mass of the projectile, only the Z_1^2 dependence of the projectile nuclear charge contributes at a fixed scaled velocity of v. For the cross sections of the double K-shell ionization, therefore, it is understood that the Z_1^4 dependence contributes at the fixed scaled energy, $E/\lambda U$.

Using the experimental cross sections, we have tried to derive a scaling law for the double K-shell ionization in the energy range where the direct Coulomb excitation is the dominant mechanism. Instead of absolute cross sections, ratios of them were used in order to avoid much of the errors in extracting the cross sections from the X-ray yields of the thick target or the uncertainty of the fluorescence yield for the double K-shell ionization. Fig. 13 shows the ratio of the double K-shell ionization cross section σ_{2K}(He) for He ion to σ_{2K}(H) for H ion bombardment. A plot of

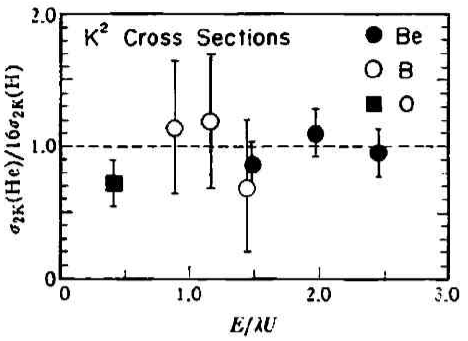

Fig. 13 Ratio of the double K-shell ionization cross sections σ_{2K} (He) for He ion to $16\sigma_{2K}$ (H) for H ion bombardment as a function of $E/\lambda U$

σ_{2K}(He)/16σ_{2K}(H) as a function of $E/\lambda U$ is a little scattered, but it is considered to be nearly constant (to be equal to unity). These facts indicate that the cross section of the double K-shell ionization by the direct Coulomb excitation obeys the scaling relation: $\sigma_{2K}/Z_1^4 = g(E/\lambda U)$. Thus, it can be said that we have for the first time succeeded in observing the Z_1^4 dependence of the double K-shell ionization cross section over a wide energy range of projectile ions.

K-shell ionization cross section for heavy ion bombardment

On the other hand, it has become clear that new and unexpected results are commonplace when the incident ions are heavy. That is, when the nuclear charge of the incident ion is not so small compared with that of the target atom, the atomic electrons of the incident ion play an

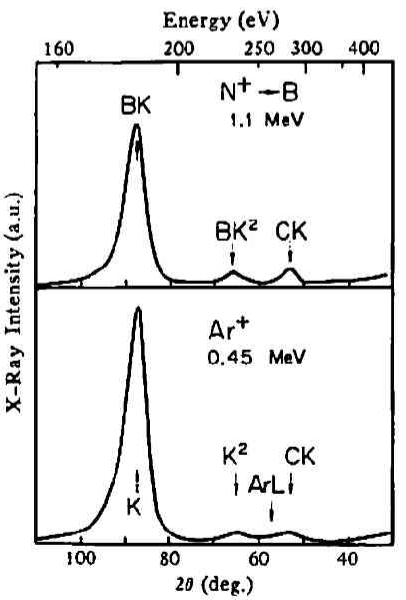

Fig .14 X-ray spectra from B target induced by 1.1 MeV N^+ and 0.45 MeV Ar^+ ion bombardment. Ar L X-ray is observed for Ar ion bombardment

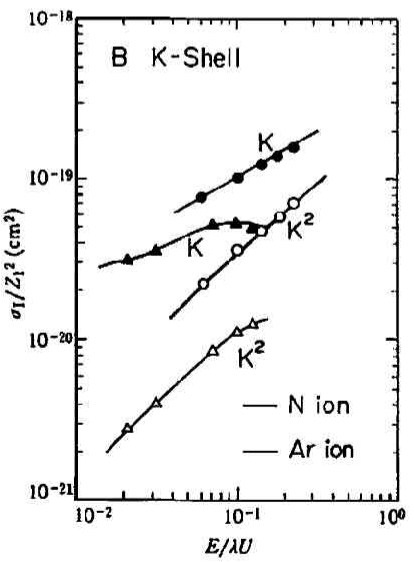

Fig. 15 Single and double K-shell ionization cross sections of B for N and Ar ion bombardment

important role in collisions[28,29]. Copious inner-shell vacancy production may occur. This vacancy production can be explained in terms of the electron promotion model presented by Fano and Lichten[3]. Fig. 14 shows the K X-ray spectra of B induced by 1.1 MeV N^+ and 0.45 MeV Ar^+ ion bombardments. The measured cross sections for the single and double K-shell ionization are summarized in Table 2 and those divided by Z_1^2 are shown in Fig. 15. The latter is a suitable value to compare the experimental data in heavy ion collisions with the theory, because the theoretical Coulomb ionization cross section is proportional to Z_1^2. The data for the heavy ions such as N and Ar ions are still some 10^2 times larger in low energies than the ionization cross sections predicted by the PWBA or the BEA theory. The large cross sections in heavy ion collisions may be understood within the framework of the Fano-Lichten model, in which inner-shell vacancies are produced as the result of electron promotion and level crossing in the quasi-molecule formed during the ion-atom collision. Fig. 16 shows the diabatic correlation diagram for the N-B and Ar-B collision systems. In the collision with N ion, B 1s electrons promote through $2p\sigma$ MO, when two atoms approach, and transitions from $2p\sigma$ to $2p\pi$ occur via rotational coupling or level crossing at zero inter-nuclear distance. The minimum distance of closest approach is reversely proportional to the incident energy

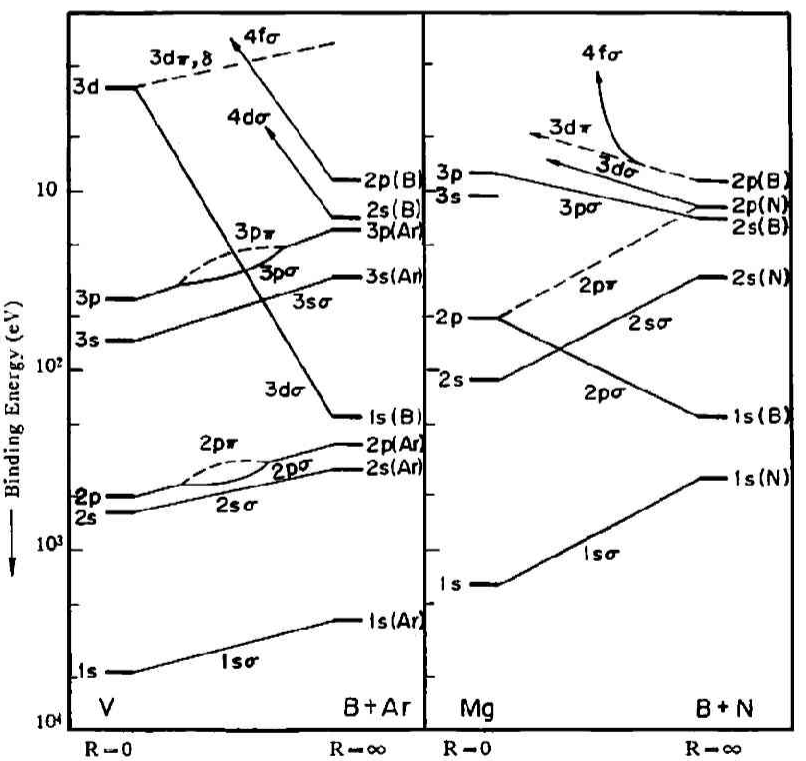

Fig. 16 Diabatic correlation diagrams for the Ar-B and N-B collision

28) H. J. Specht, *Z. Physik*, **185**, 301 (1965)
29) F. W. Saris, *Physica*, **52**, 290 (1971)

of the projectile ion. In N ion bombardment, the measured cross sections of the K-shell ionization increase with increasing energy of the incident projectile and the ratio of the cross sections for the double K-shell to the single K-shell ionization is larger at high energy. These facts support the expectation that the ionization cross section depends strongly on the incident energy of the projectile ions in excitation by rotational coupling. The very dissimilar behavior of Ar ion bombardment, that is, rather energy-independent cross section, is suggested to be due to the difference of the electron promotion mechanism with that in the case of another ions studied. In Ar ion bombardment, B 1s electrons promote through $3d\sigma$ MO and probably through several level crossings of $3d\sigma$ MO with higher levels, as shown in Fig. 16. The measured cross sections for the single K-shell ionization show little energy dependence. This may be explained by the succesive level crossings of $3d\sigma$ MO, when the Ar ion approaches the B atom. However, it is not clear why the cross sections for the double K-shell ionization show strong energy dependence. Thus, the experimental results for heavy ion-atom collisions support the theory that inner-shell vacancies are produced as the result of electron promotion and level crossings in the quasi-molecule formed during ion-atom collisions.

Acknowledgment

The author is grateful to Prof. J. Osugi for his interest and helpful advices in this work and for critical reading the manuscript. The author is indebted to Dr. K. Ozawa, Prof. F. Fujimoto, Dr. M. Terasawa and Dr. K. Komaki for their valuable suggestions and discussions throughout this work, and to Dr. S. Tsujimura and Dr. K. Izui for their continuous interest. The author also wishes to thank Mr. C. Kobayashi and Mr. S. Kanda for their kind operation of the 2-MV Van de Graaff accelerator.

Solid State Chemistry Laboratory
Division of Chemistry
Japan Atomi Energy Research Institute
Tokai-Mura, Ibaraki 319-11
Japan